RESPONSE OF A BRIDGE AND ITS SUBSOIL TO GROUND SHAKING

by

Toshiro Fujiwara and Jun Kawamata[I]

SYNOPSIS

Response of a railway truss girder bridge with its surrounding ground in an earthquake swarm occured in the central part of Japan from 1965 to 1968 has been observed. Meanwhile, cyclic loading tests, seismic prospecting of subsoil and others were carried out. Comparison of the results of these measurements with the earthquake response analysis data on bridge structure has made it almost clear why bridge and other structures can survive with little damage even an earthquake of large acceleration when it is one of a shock type with higher frequency components than the proper frequency of structure.

INTRODUCTION

The earthquake response of a structure is said to vary widely, depending on the nature of input seismic wave and the dynamic characteristics of its subsoil. Thus it is essential in the investigation of this response to get a full grasp of the dynamic characteristics respectively of the earthquake, the ground and the structure and their interactions.

The Matsushiro Earthquake Swarm which happened in the central part of Japan over a period of 1965-1968 offered an appropriate opportunity to investigate these interactions and check them against the observation data. The features of this earthquake swarm were such that the foci were extremely shallow, being 0-10 Km depths and the earthquake was of a shock type of short period and short duration. It is for this reason that, in spite of the earthquake being one of an extremely high acceleration, about 500 gals on the ground surface, all the railway structures suffered little damage and none of them collapsed, but it should be noted that this earthquake swarm has revealed that, depending on the nature of the seismic wave, the response behavior of a structure is exceedingly variable.

After 1967, we had a chance to carry out earthquake observations with a railway bridge built over the river Chikuma flowing through this district. Later we have been able to investigate the dynamic characteristics of this bridge and its subsoil through cyclic loading, seismic prospecting and others. (See Ref. 1)

The bridge, 457 m in the total length, is composed of one 19.2 m and eight 22.3 m spans of deck plate girders (each with caisson, 4 m diameter 10 m long): and four 62.4 m spans of through truss girders (with caisson, 5.5 m diameter 17 m long): it has been erected in 1961.

I Structure Laboratory, Railway Technical Research Institute, Japanese National Railways.

As indicated in Fig.1, it is situated about 6 Km from Matsushiro-cho, which is supposed to be the epicenters in 1967. Figure 2 is a schematic view of the bridge and Fig.3 (a) gives an outline of the local geology. The ground involved is an alluvial plain developed along the river in the valley, it being mainly composed of sands and gravels, and partially of sand layers interlarded with thin clay layers.

EARTHQUAKE OBSERVATION AND GROUND SURVEY

Earthquake observations were made at 11 spots in total, including 5 spots on the truss girders of the bridge and 6 spots underground in the vicinity. The longitudinal axis and the normal direction to it in this bridge agree respectively with NS and EW approximately. All the measuring points are shown as Fig.4.

Eight measuring components in all were taken on the bridge: two at the top of the No.10 pier (G-point): one at the top of the No.10 caisson (J-point): two each at the tops of the No.11 pier (H-point) and the No.11 caisson (I-point): and one at the downstream cross beam end at mid-span between the No.10 and No.11 piers (K-point). With the single component a horizontal acceleration in the direction normal to the longitudinal axis of the bridge was registered, while with the double components horizontal accelerations in both the longitudinal axis direction and the direction normal to it were registered.

The spots for underground measurements were selected on the dry river bed 55 m far from the bridge so that they might be as free from the effect of bridge vibration as possible. One seismograph each was set at the bottom of four boring holes, the depth of setting and the number of components measured being as follows: 30.0 m (A-point) three: 16.6 m (B-point) two: 10.0 m (C-point) two: and 4.0 m (D-point) three. The two components were NS and EW: and the three were UD as well as NS and EW.

Meanwhile, two components were set at a depth of 10.0 m (E-point) and two more at a depth of 3.8 m (F-point), 2.5 m downstream of the No.10 caisson. Thus the underground measuring spots totaled 14.

The seismographs set underground were turned by manipulating a cable attached thereto from the ground surface so that their pendulums might correctly oscillate in the direction of NS and EW. The azimth was decided from the ground surface using a magnetic compass and a photoelectric element built into the seismograph.(See Ref. 2)

To avoid being falsely started under train passage, the recorder was so arranged using the output of the UD component in the seismograph at the deepest point (A-point) that it could be started only when the seismic waves reached a certain acceleration level.

The recording time was arbitrarily set by the timer, while the time of commencement of shaking was registered by the clocking-printer. The seismograph used had an constant overall acceleration sensitivity in the range of 0.3-30 Hz and a natural period of 0.26 sec. Figure 5 shows seismographs as set underground.

Ground survey was executed by seismic prospecting with blasting and plate hammering. The subsoil structures expressed in terms of P-wave and S-wave velocities thus measured is illustrated in Fig.3 (b). Some correspondence can be recognized between Fig.3 (a) and (b). It has been ascertained in time of boring the A-point and others that the deposite with an S-wave velocity of 470 m/sec extends nearly similar at least to a depth of 30 m. Some vibration tests were made at the H-point on the ground surface.

ANALYSIS OF OBSERVATION DATA

Table 1 lists the maximum acceleration readings at respective measuring points in 29 earthquakes recorded. From these data, the ratio of maximum acceleration with reference to the D-point was found for each point. The values given in Fig.6 are the average and variation width of this ratio for each point. The average of this ratio generally tends to become larger from depth to surface, but at depths greater than 10 m the value settles to 0.5-0.6. This fact seems to verify the results in Fig.3 that the subsoil structure at such a depth is nearly homogeneous. It is obvious that the value of this ratio sharply drops in the bedrock at depths greater than 30 m. At points less than 10 m deep the ratio is 0.6-1.0 for the existence of discontinuous layers as illustrated in Fig.3. It should be noted here that at the E- and F-points near the caisson, the average of this ratio turned out about 20 % higher than at the C- and D-points which were removed from the bridge and located at the similar depth as E and F respectively. The values of this ratio registered on the bridge increased as follows: 1.0-1.6 at the caisson top, 2.0-2.3 at the pier top and 3.0 at cross-beam.

Figure 7 shows how the maximum acceleration of response at the pier top changes depending on the maximum acceleration on and beneath the ground. The acceleration of the pier top does not seem to become correspondingly large even if the acceleration of the ground is large. This might be such reason as the follows: horizontal or elastic motions set off against rocking motions of the pier when the intensity of earthquake becomes larger. Such a relation is also verified by similar observation data with the filling though the causes may be different each other.

Fourier spectra of main motions in the earthquake records turned out as Figs.8, 9 and 10. Figure 8 compares three earthquakes recorded at the A-point 30 m deep underground: one of them with a sharp decline of the frequency components exceeding 5 Hz had its epicenter located far away, and the other two belonged to the Matsushiro Earthquake Swarm mentioned above. This is quite natural in view of the Matsushiro Earthquake Swarm being earthquakes happening with epicenters near by in which the high-frequency components predominate. A peak of about 1-2 Hz appearing a little in the figure may be attributable to the deep subsoil structure.

Figure 9 compares four spots of ground with different depths: A, B, C and D. A peak of about 3-5 Hz is seen somewhat in the figure. It is not distinct at the A- and B-points, but conspicuous at the C- and D-points.

It might be the predominant frequency of the surface layer. But on the other hand, the predominant frequency of the surface layer as obtained from the result in Fig.3 (b) or the ground-vibration tests is close to 5 Hz. It will need further checking to judge that these two frequencies originate from the same surface layer. Figure 10 is a comparison between the E- and F-points near the No.10 caisson and the G- and J-points at the top of the same pier and caisson.

The peak of 3-4 Hz is likely to be affected by the interaction between ground and bridge. The reason for this can be explained from the values of spectra diminishing in the following order: G and J > F > E at 3-4 Hz, and from the proper frequency of first order of the substructure being set at 2.82 Hz in the next chapter.

EARTHQUAKE RESPONSE ANALYSIS FOR BRIDGE SUBSTRUCTURE

Using the above-mentioned earthquake records, the earthquake response of the No.10 pier with caisson in the direction normal to the longitudinal axis has been analysed. The dimensions of the caisson, pier and girder of the bridge are given in Fig.11(a) and their analysis model is shown in Fig.11(b). As shown in the figure, the motion of an 8-mass system considering the stiffness of each part and the layout of earthquake measuring points may generally be expressed by the following equation:

$$M\ddot{X} + C\dot{X} + KX = P(t) \qquad (1)$$

where M, C and K are respectively the mass matrix, the damping matrix and the stiffness matrix: X is the deformation of joint, P is the acting seismic force: and $\ddot{X}$ and $\dot{X}$ are respectively the second derivative and the first derivative of X with respect to time t.

The response calculations of the rocking and bending motion, with the shear deformation and rotational inertia ignored and the linear response and viscus damping assumed, were carried out by using equation (1). Table 2 lists the sectional properties of members as adopted for this calculations, based on supposedly appropriate assumptions and measured data.

The natural frequencies and modes thus calculated are given in Fig.12: some typical response waveforms of the joints as compared with observed data in Fig.13: and the response waveforms as compared with the typical major earthquakes such as El Centro 1940 and Tokachioki 1968 in Fig.14.

From Fig.12 it is seen that the natural frequencies of the first and the second order of the substructure are respectively 2.82 Hz and 9.08 Hz: and those of the girders are respectively 1.59 Hz and 6.27 Hz. Meanwhile, Fig.13 seems to show that there is fairly good agreement at least in the frequency between the calculated displacement and the displacement estimated from the measured acceleration. This shows that the spring constants given here explain considerably the measured data. In comparing the amounts of displacement it would be necessary to be careful in choosing the damping constants.

Figure 14 indicates how widely the waveforms of response displacement vary depending on the input seismic waves. If the maximum input seismic acceleration is set at the same value, i.e., 100 gals, the maximum response displacement in the Matsushiro Earthquake will be less than that in the El Centro Earthquake or the Tokachioki Earthquake.

From this it is understood that in the Matsushiro Earthquake the No.10 pier with caisson resonated to a small extent since the power near the proper frequency of substructure is low for the seismic components with high frequencies, and accordingly it did not collapse.

These results of analysis will make comparison with the design values an interesting study.

CYCLIC LOADING TEST OF BRIDGE AND ITS RESULTS

The No.10 pier, at the top of which a small vibrator was set, was submitted to cyclic loading in the direction normal to the longitudinal axis. The vibrator was of an eccentric weight type with a maximum shaking capacity of 1 ton-g, but it could not be given full play. The resonance curves plotted from the results of the test are illustrated in Fig.15. The resonance point of the pier is ambiguous in this figure, but peaks of 3.3-3.4 Hz and 9.6-9.7 Hz have been registered at the points No.3 and No.7 of the mid-span.

These values seem to correspond with F2 (2.82 Hz) and F4 (9.08 Hz) above calculated. Fig.16 illustrates the Fourier spectra of three earthquakes at the K-point: in this case, too, a conspicuous peak occurs at about 3 Hz, and the peak 9.6-9.7 Hz cannot be considered to represent an earthquake with a distant epicenter.

CONCLUSIONS

From multipoint earthquake observations of bridge and ground, the vertical distributions from ground to pier of maximum acceleration have been obtained. Naturally, the maximum acceleration tends generally to increase from depth to top with a significant amplification at each spot.

In a major earthquake the top of pier is not likely to develop such a large amplified acceleration as extrapolated from the data on minor earthquakes.

Checking of the earthquake response analysis data against the measured data has elucidated why the bridge suffers little damage in an earthquake of a shock type with a large value of maximum acceleration but without a similar frequency component to the proper frequency of bridge.

Response of a bridge varies widely depending on the input seismic waveforms. The frequency characteristics inherent in the seismic motion, the predominant frequency of the ground, and the natural frequency of a bridge, are intricately compounded to decide the scale of bridge vibration in earthquake.

REFERENCES

1) Fujiwara T. (1968), On behavior of railway bridge with well-type foundation during earthquakes. A report in JNR.
2) Fujiwara T. and T. Oda (1966), On seismometers setting in bore-hole of Seto Inland Sea of Japan. Proc. Japan Earthq. Eng. Symp. 1966, 133/138.

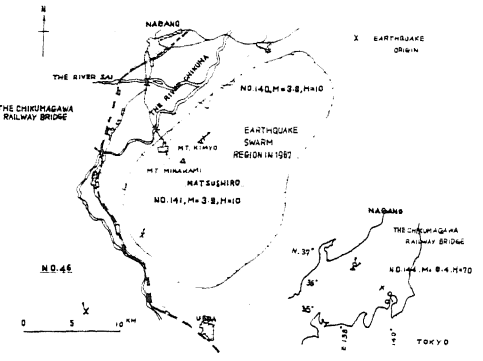

Fig. 1 Location of the bridge and Matsushiro Earthquake Swarm region in 1967.

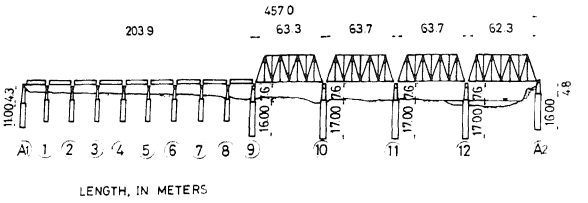

Fig. 2 Schematic view of the Chikumagawa railway bridge.

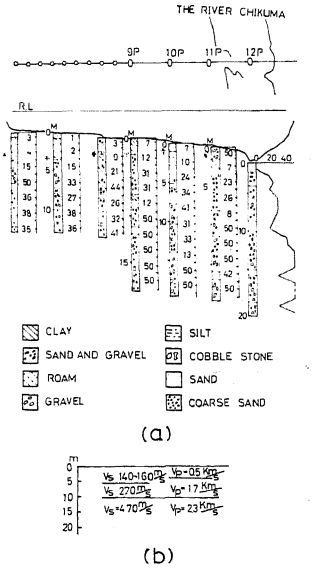

Fig. 3 (a) Geological formation, values except depths show penetration resistance, (b) Subsoil structures by P- and S-waves.

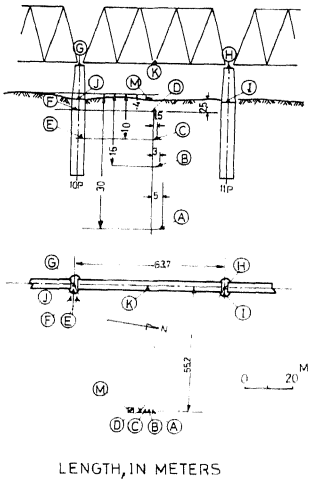

Fig. 4 Earthquake observation points at the bridge site.

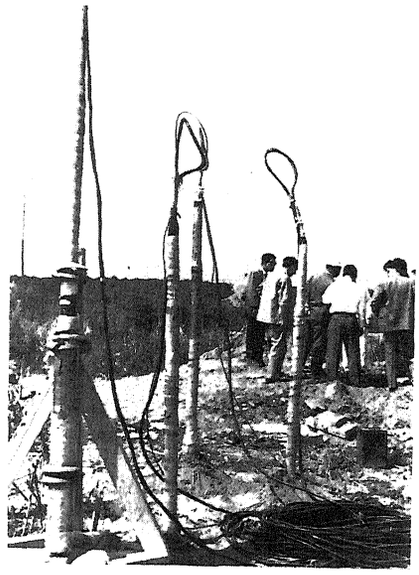

Fig. 5 Bore-hole seismographs.

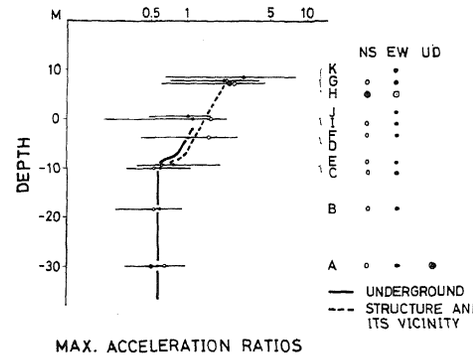

Fig. 6 Vertical distribution of maximum acceleration ratios.

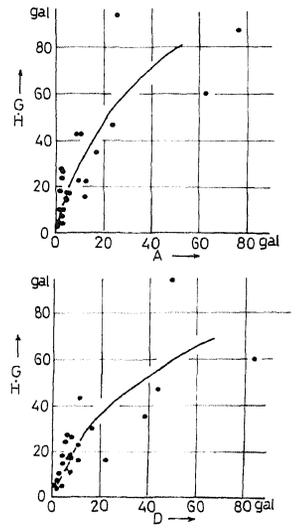

Fig. 7 Relations between piers (G,H) and ground (A,D) in the maximum acceleration of earthquake.

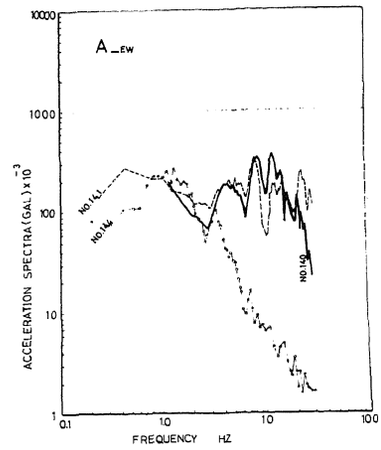

Fig. 8 Fourier spectra of three different earthquakes at the point A.

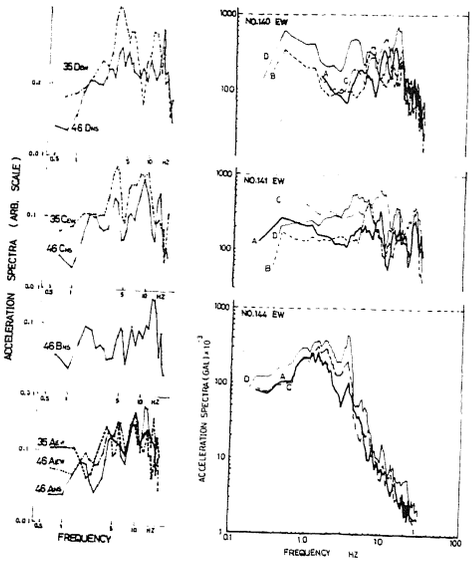

Fig. 9 Fourier spectra of some earthquakes at the points A, B, C and D.

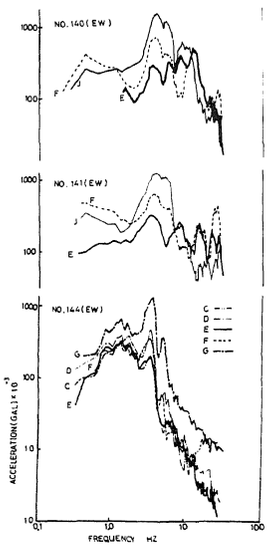

Fig. 10 Fourier spectra of three earthquakes at the points E, F, J and G.

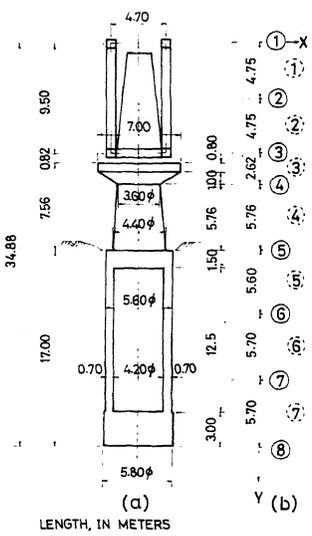

Fig. 11 (a) No.10 pier with caisson, (b) An analysis model, ○ shows joint number and ⬡ member number.

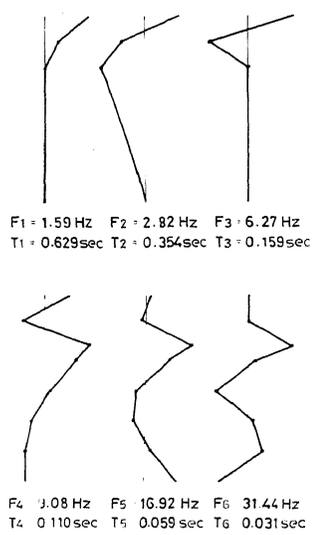

Fig. 12 Natural frequencies and modes of No.10 pier in lateral direction.

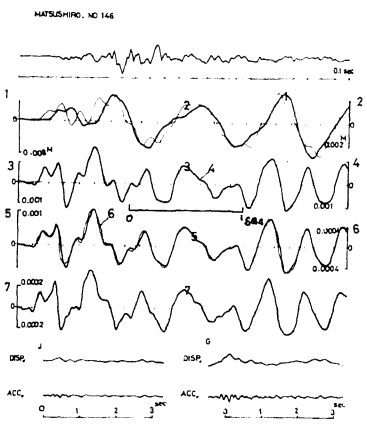

Fig. 13 Calculated and observed response waveforms of displacement at each joint of No.10 pier when its caisson-base is hit by the earthquake No.146 (B-point). Top one shows the input earthquake, its maximum being 100 gals, middle seven the response calculated and the lowest four the response observed at J-point (No.5) and G-point (No.3): In these four, DISP. is displacement calculated from accelerograms (ACC.).

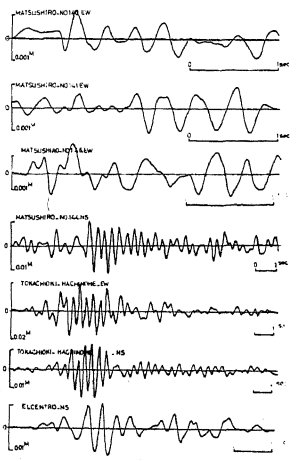

Fig. 14 Calculated response waveforms of displacement at No.3 joint of No.10 pier caused by six earthquakes with their input maximum acceleration 100 gals. 1 sec represents the interval of 1 sec.

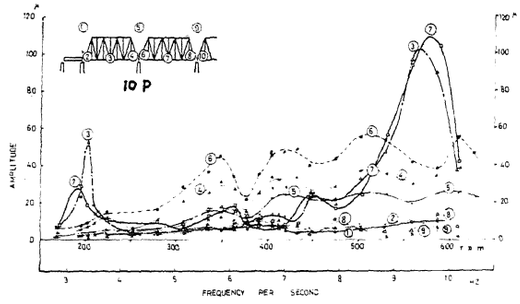

Fig. 15 Resonance curves obtained under cyclic loading.

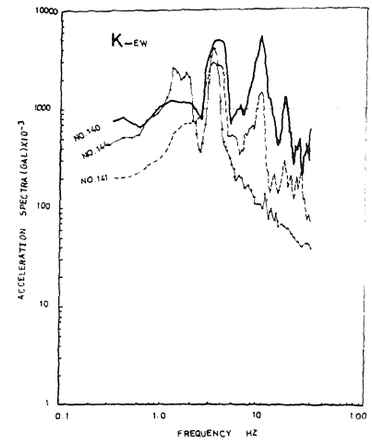

Fig. 16 Fourier spectra of three earthquakes at the point K.

TABLE 1

MAXIMUM EARTHQUAKE ACCELERATION IN CM/SEC^2 AT EACH OBSERVATION POINT

Earthq. No.	Time of occurrence M	D	H	M	a_1	a_2	a_3	a_4	a_5	a_6	a_7	a_8	a_9	a_{10}	a_{11}	a_{12}	a_{13}	a_{14}	a_{15}	a_{16}	a_{17}	a_{18}	a_{19}	a_{20}	a_{21}
1	1962	6	19	12	29	4.2	2.9	1.9	4.3	2.4	3.3	2.6	10.9	4.8	2.2	4.3	4.3	12.6	5.0	12.4	11.2	12.0	7.0	6.8	4.2	17.3
2	1962	7	19	18	24	4.2	4.2	-	4.1	3.0	3.1	3.3	3.3	1.6	3.3	3.9	4.1	10.4	10.0	10.6	14.0	8.4	15.3	7.0	5.0	7.2	25.3
3	1962	6	24	01	31	3.0	1.5	0.6	1.1	1.4	0.9	1.3	1.3	1.4	1.3	1.1	1.0	2.3	1.4	3.0	3.4	3.2	3.4	2.0	2.0	-	-
4	1962	6	24	21	31	1.4	1.2	0.4	1.1	1.4	0.9	1.3	3.0	2.8	1.2	1.1	1.1	3.0	2.0	3.3	3.1	3.3	3.3	2.0	-	-	-
5	1962	7	17	11	32	3.4	2.4	-	1.5	1.4	1.8	2.3	4.7	3.8	2.3	1.8	2.1	7.3	3.2	6.0	4.0	3.6	5.4	2.4	2.0	-	3.2
16	1962	7	18	07	31	3.4	3.9	-	3.0	3.7	2.1	2.4	7.7	5.2	3.4	2.4	2.7	7.9	5.2	12.6	12.2	17.0	16.8	9.0	10.4	8.3	25.0
17	1962	7	21	02	35	2.7	2.7	-	1.3	-	2.4	2.4	6.4	4.4	2.7	2.0	2.4	10.2	7.7	18.0	15.0	18.0	17.4	10.0	10.0	7.8	25.0
20	1962	7	24	07	06	3.4	3.1	-	2.4	-	2.0	2.8	5.4	3.8	3.8	-	2.4	10.2	8.0	15.0	14.0	17.0	16.8	9.8	-	4.8	22.8
20-1	1962	7	24	07	08	3.4	2.8	-	2.4	-	2.0	2.8	5.4	3.8	3.8	-	-	-	-	-	-	-	-	-	-	-	-
21	1962	7	24	22	33	3.4	-	-	2.4	-	3.3	3.1	8.3	-	4.3	-	-	-	-	13.2	10.2	18.0	18.2	11.2	-	6.7	-
23	1962	7	24	23	35	3.4	2.0	0.8	2.4	-	2.4	2.4	6.4	3.8	3.8	-	2.0	-	4.8	8.0	5.4	10.8	9.2	8.4	6.4	5.4	11.3
24	1962	7	24	16	19	2.4	1.9	0.8	2.3	-	1.4	1.8	4.8	3.2	1.3	3.4	2.4	3.4	3.0	10.0	11.4	15.0	9.8	9.4	5.4	11.3	30.0
32	1962	8	14	07	17	2.4	1.9	-	2.2	-	2.0	1.7	-	1.2	-	2.4	-	13.4	-	15.4	-	15.4	-	43.4	-	40.0	12.4
32-1	1962	8	14	03	04	1.4	2.4	-	1.3	-	-	-	2.8	-	-	1.9	-	4.3	-	3.8	-	7.0	-	3.0	-	-	-
37-1	1962	9	11	13	05	2.4	3.3	-	2.7	-	3.2	-	5.8	-	4.7	-	8.8	-	19.2	-	24.3	-	17.3	-	-	-	-
40	1962	9	16	23	52	17.8	10.3	-	3.8	-	10.5	-	21.3	-	-	-	-	-	-	-	-	-	-	-	-	-	-
44	1962	9	18	23	37	11.0	7.4	-	4.2	-	8.0	-	11.8	-	14.0	-	19.7	-	44.5	-	28.3	-	7.4	-	-	-	42.5
44-1	1962	10	14	03	03	8.7	15.3	-	4.7	-	9.4	-	11.8	-	9.0	-	15.8	-	19.3	-	22.3	-	11.8	-	-	-	33.5
44-2	1962	10	14	04	48	8.2	5.1	1.4	-	2.9	-	3.3	-	7.4	-	-	6.0	-	2.7	-	8.3	-	16.4	-	2.3	-	-
44-3	1962	10	14	04	48	8.2	5.1	1.4	-	2.9	-	3.3	-	18.8	-	-	10.0	-	10.9	-	-	-	-	-	10.0	-	50.5
44-4	1962	10	14	04	48	3.0	2.0	1.4	-	2.9	-	2.3	-	6.0	-	-	13.4	-	18.8	-	25.5	-	27.0	-	8.7	-	50.5
75-2	1962	12	27	03	46	43.2	44.0	39.8	-	46.0	-	46.3	-	86.0	-	-	38.3	-	63.6	-	68.0	-	50.0	-	19.6	-	94.5
107	1963	3	11	11	30	5.3	10.0	-	4.9	5.4	10.3	-	16.3	-	-	-	7.0	-	8.0	-	22.1	-	30.0	-	8.0	-	75.0
108	1963	3	12	05	20	17.2	17.2	-	10.8	17.4	14.0	19.0	22.8	38.8	-	-	-	-	22.4	-	27.0	-	27.0	-	11.0	-	55.5
109	1963	3	18	09	01	-	-	-	-	-	-	-	-	-	-	-	14.4	-	22.4	-	27.0	-	35.0	-	11.0	-	55.5
75-1	1963	3	20	06	32	16.2	26.6	-	8.4	22.0	11.8	32.3	44.4	-	-	-	18.0	-	35.6	-	36.0	-	56.0	-	19.2	-	55.0
75-2	1963	3	20	06	32	23.4	22.4	-	10.8	22.0	22.0	32.3	44.4	-	-	-	20.4	-	31.0	-	66.0	-	56.0	-	20.4	-	77.0
75-3	1963	3	20	06	32	10.0	15.6	-	7.8	15.6	8.2	16.3	16.3	32.4	-	-	12.8	-	20.0	-	46.0	-	42.0	-	14.4	-	39.5

Earthq. No.	a_{22}	a_{23}	a_{24}	a_{25}	a_{26}	a_{27}	a_{28}	a_{29}	a_{30}	a_{31}	a_{32}	a_{33}	a_{34}	a_{35}	a_{36}	a_{37}	a_{38}	a_{39}	a_{40}	a_{41}	a_{42}	a_{43}	a_{44}	a_{45}
1	4.2	12.6	5.0	12.4	11.2	12.0	7.0	6.8	4.2	17.3	-	-	-	-	-	-	-	-	-	-	-	-	-	-
2	10.0	10.6	14.0	8.4	15.3	7.0	5.0	-	7.2	25.3	-	-	-	-	-	-	-	-	-	-	-	-	-	-
3	1.4	3.0	3.4	3.2	3.4	2.0	2.0	-	-	-	-	-	-	-	-	-	-	-	-	-	-	-	-	-
4	3.3	3.3	3.1	3.3	3.3	2.0	-	-	-	-	-	-	-	-	-	-	-	-	-	-	-	-	-	-
5	3.2	4.0	4.0	3.6	5.4	2.4	2.0	-	3.2	-	-	-	-	-	-	-	-	-	-	-	-	-	-	-
16	5.2	12.6	17.0	17.0	16.8	9.0	10.4	-	8.3	25.0	-	-	-	-	-	-	-	-	-	-	-	-	-	-
17	5.2	18.0	15.0	18.0	17.4	10.0	10.0	-	7.8	25.0	-	-	-	-	-	-	-	-	-	-	-	-	-	-
20	8.0	15.0	14.0	17.0	16.8	9.8	-	-	4.8	22.8	-	-	-	-	-	-	-	-	-	-	-	-	-	-
20-1	-	-	-	-	-	-	-	-	-	-	-	-	-	-	-	-	-	-	-	-	-	-	-	-
21	-	13.2	10.2	18.0	18.2	11.2	8.4	-	6.7	-	-	-	-	-	-	-	-	-	-	-	-	-	-	-
23	-	8.8	8.0	5.4	10.8	9.2	8.4	-	5.4	11.3	-	-	-	-	-	-	-	-	-	-	-	-	-	-
24	3.4	10.0	11.4	15.0	9.8	9.4	5.4	-	11.3	30.0	-	-	-	-	-	-	-	-	-	-	-	-	-	-
32	-	-	13.4	-	43.4	-	40.0	12.4	-	-	-	-	-	-	-	-	-	-	-	-	-	-	-	-
32-1	-	3.3	-	7.0	-	3.0	-	-	-	-	-	-	-	-	-	-	-	-	-	-	-	-	-	-
37-1	-	8.8	-	19.2	-	24.3	-	17.3	-	-	-	-	-	-	-	-	-	-	-	-	-	-	-	-
40	-	-	-	-	-	-	-	-	-	-	-	-	-	-	-	-	-	-	-	-	-	-	-	-
44	14.0	-	19.7	-	44.5	-	28.3	-	7.4	-	-	-	-	-	-	-	-	-	-	-	-	-	-	-
44-1	9.0	-	15.8	-	19.3	-	22.3	-	11.8	-	-	-	-	-	-	-	-	-	-	-	-	-	-	-
44-2	-	6.0	-	2.7	-	8.3	-	16.4	-	2.3	-	-	-	-	-	-	-	-	-	-	-	-	-	-
44-3	-	10.0	-	10.9	-	-	-	-	-	10.0	-	-	-	-	-	-	-	-	-	-	-	-	-	-
44-4	-	13.4	-	18.8	-	25.5	-	27.0	-	8.7	-	-	-	-	-	-	-	-	-	-	-	-	-	-
107	-	38.3	-	63.6	-	68.0	-	50.0	-	19.6	-	-	-	-	-	-	-	-	-	-	-	-	-	-
108	-	7.0	-	8.0	-	22.1	-	30.0	-	8.0	-	-	-	-	-	-	-	-	-	-	-	-	-	-
109	-	14.4	-	22.4	-	27.0	-	35.0	-	11.0	-	-	-	-	-	-	-	-	-	-	-	-	-	-
75-1	-	18.0	-	35.6	-	36.0	-	56.0	-	19.2	-	-	-	-	-	-	-	-	-	-	-	-	-	-
75-2	-	20.4	-	31.0	-	66.0	-	56.0	-	20.4	-	-	-	-	-	-	-	-	-	-	-	-	-	-
75-3	-	12.8	-	20.0	-	46.0	-	42.0	-	14.4	-	-	-	-	-	-	-	-	-	-	-	-	-	-

TABLE 2

THE CONSTANTS OF NO.10 PIER WITH CAISSON

SECTIONAL PROPERTIES OF MEMBER

MEMBER NO.	SECTIONAL AREAS (M^2)	YOUNG'S MODULUS (TON/M^2)	MOMENT OF INERTIA (M^4)
1	1.3765	21000000	0.004034
2	1.3765	21000000	0.004034
3	19.467	3000000	84.856
4	12.693	3000000	13.514
5	14.487	3000000	17.092
6	10.776	3000000	35.001
7	19.010	3000000	44.869

SPRING CONSTANTS

SUPPORT NO.	HORIZONTAL SPRING CONSTANTS (TON/M)	VERTICAL SPRING CONSTANT (TON/M)	ROTATIONAL SPRING CONSTANT (TON-M/RAD.)
5	27440	-	-
6	28918	-	-
7	61197	-	-
8	68696	-	531056

WEIGHT OF JOINT

JOINT NO.	WEIGHT OF JOINT (TON)
1	26.9
2	93.2
3	113.4
4	134.2
5	626.7
6	1073.9
7	1104.3
8	569.9